Control over Wettability of Textured Surfaces by Electrospray Deposition

Tomoya Mizukoshi,[1,2] Hidetoshi Matsumoto,[1,2] Mie Minagawa,[1,2] Akihiko Tanioka[1,2]

[1]*Department of Organic and Polymeric Materials, Tokyo Institute of Technology, Meguro-ku, Tokyo 152-8552, Japan*
[2]*International Research Center of Macromolecular Science, Tokyo Institute of Technology, Meguro-ku, Tokyo 152-8552, Japan*

Received 7 April 2006; accepted 1 August 2006
DOI 10.1002/app.25191
Published online in Wiley InterScience (www.interscience.wiley.com).

ABSTRACT: Microtextured surfaces were prepared by electrospray deposition (ESD) from hydrophilic and hydrophobic acrylic resin solutions. The surface morphologies and topologies were characterized using scanning electron microscopy and laser profile microscopy, respectively. Wetting behaviors on the surfaces were characterized by contact angle and sliding angle measurements. The contact angle of the water droplet on the hydrophilic resin-coated surfaces decreased with an increase in the surface roughness. On the other hand, the contact angle on the hydrophobic resin-coated surfaces increased with an increase in the surface roughness. In addition, a patterned surface composed of aligned fibers by ESD showed anisotropy of both wetting and sliding behaviors. These results indicate that ESD is a useful method for designing a textured surfaces and controlling the surface wettability. © 2006 Wiley Periodicals, Inc. J Appl Polym Sci 103: 3811–3817, 2007

Key words: microstructure; surfaces; coatings

INTRODUCTION

Electrospray deposition (ESD) is a straightforward and versatile method for forming thin films. This method has the following advantages: (i) applicability for broad spectrum of molecules such as: inorganic molecules, synthetic polymers, proteins, and DNA; and (ii) ability to deposit polymer thin films with nano-microscaled structures, which range from spheres to fibers under atmospheric pressure.[1–10] Electrospray-deposited thin films have recently attracted much attention for applications such as biosensors and biochips (e.g., protein/DNA-microarrays and microfluidic devices), antifouling or biocompatible coatings for medical devices, high-performance filter media, drug delivery systems, and biomaterial scaffolds for tissue engineering.[1–10] The ESD methods consist of the following steps: (i) a strong electric field is applied between a nozzle containing the polymer solution and a conductive substrate, (ii) when the voltage reaches a critical value, electrostatic forces overcome the surface tension of the solution, (iii) charged droplets (or jets) are sprayed from the tip of the nozzle, in a dry atmosphere; and (iv) the dried droplets (or jets) are finally collected on the substrate to form a thin film.

One major advantage of the ESD technology is the forming of nano-microtextured surfaces.[11–13] Not only the surface chemical composition, but also the surface roughness affects the wetting behavior.[14] Textured surfaces have been produced by a range of chemical and physical methods: electrochemical polymerization,[15] sol–gel method,[16] electrodeposition,[17] photolithography,[18] micromolding,[19] and so forth.[20–22] Recently, some researchers have shown that the electrospray process is useful for producing superhydrophobic surfaces.[23–27] However, there have been few systematic studies on the relationship between the morphology of the electrosprayed surface and the wetting behavior.

In the present study, we prepared microtextured surfaces by ESD and then characterized their morphology and wettability. We used hydrophilic and hydrophobic acrylic resins, poly(2-hydroxyethyl methacrylate-*co*-methacrylic acid) and poly (methyl methacrylate-*co*-butyl methacrylate-*co*-2-hydroxyethyl methacrylate-*co*-methacrylic acid), as the coating polymers. The objectives of the present investigation are (i) to prepare microtextured surfaces by ESD, and (ii) to identify the effect of the surface morphology on the wettability.

EXPERIMENTAL

Materials

Poly(2-hydroxyethyl methacrylate-*co*-methacrylic acid) (poly(2-HEMA-*co*-MAA), 2-HEMA/MAA = 75/25 in molar ratio, M_W = 100,000) and poly(methyl methacrylate-*co*-butyl methacrylate-*co*-2-hydroxyethyl methacrylate-*co*-methacrylic acid) (poly(MMA-*co*-BMA-*co*-2-

Correspondence to: A. Tanioka (atanioka@o.cc.titech.ac.jp).

TABLE I
Properties of Poly(2-HEMA-*co*-MAA)/MeOH Solution

Concentration (wt %)	Viscosity (mPas)	Surface tension (mN/m)	Conductivity (mS/m)
10	3.41	24.7	1.37
15	8.16	24.2	1.75
20	24.3	24.6	2.01
30	94.2	24.7	2.06

HEMA-*co*-MAA), MMA/BMA/2-HEMA/MAA = 50/25/24/1 in molar ratio, M_W = 120,000) were used as the hydrophilic and hydrophobic resins, respectively. These acrylic resins were obtained from Mitsubishi Chemical MKV Company, Japan. Methanol (MeOH) of HPLC grade and 2-propanol (IPA) of extra-pure grade were purchased from Wako Pure Chemical, Japan. All reagents were used without further purification. Aluminum plates (AL-013Series, Nilaco, Japan) were used as the substrate.

Solution properties

The solution viscosities were measured by an oscillating-type viscosity meter (VM-100A, CBC Materials, Japan). Surface tensions of the solution were determined by the Whilhelmy plate method using a fully automated surface tensiometer (CBVP-Z, Kyowa Interface Science, Japan). The solution conductivities were measured using a conductivity meter (CM-20S, TOA, Japan) with conductivity cell (CG-511B, TOA, Japan). All measurements were carried out at 25°C.

Fabrication of microtextured surfaces by ESD

The ESD device is the same as that used in a previous study.[10] The polymer solution was contained in a syringe with a stainless-steel nozzle (1.0 mm internal diameter). The nozzle was connected to a high-voltage regulated DC power supply (HDV-20K 7.5STD, Pulse Electronic Engineering, Japan). A constant volume flow rate was maintained using a syringe-type infusion pump (MCIP-III, Minato Concept, Japan). The grounded substrate was an aluminum plate (15 × 20 cm^2 area). The distance between the nozzle tip and the substrate surface was 15 cm, the applied voltage was 15 kV (corresponding to an applied field of 1.0 kV/cm), and the flow rate was 0.02 mL/min. The duration of the deposition was 20 min, which is sufficient to obtain the coating layer with a stable surface structure. All sprayings were carried out at 25°C under 30% relative humidity.

Observation of surface morphology

The morphologies of the microtextured surfaces were observed using a scanning electron microscope (SEM, SM-200, Topcon, Japan) operated at 10 kV. All samples were sputter-coated with Au. The surface roughness R_a (average deviation from the arithmetic centerline) of the microtextured surfaces was determined using a color 3D profile microscope (VK-9500, KEYENCE, Japan). A violet laser with a 408 nm wavelength was used as the incident beam. The observation area was 270 μm × 202 μm.

Evaluation of wetting behavior

The static contact angles of the water droplets were measured by the sessile drop method using a contact angle measurement system (DropMaster 500, Kyowa Interface Science, Japan). The weight of the water droplets for the measurements was 2 mg. All measurements were carried out at five or more different points for each sample at 25°C. The sliding angles of the water droplets were measured using a fully automated sliding angle measurement system (Drop Master 700 and DM-SA, Kyowa Interface Science, Japan). The weight of the water droplets for the measurements was varied from 10 to 50 mg. All measurements were carried out at five or more different points for each sample at 25°C.

RESULTS AND DISCUSSION

Morphology and wettability of microtextured surfaces by ESD

The properties of the coating solutions, hydrophilic acrylic resin/MeOH solution and hydrophobic acrylic resin/IPA solution, are summarized in Tables I and II, respectively. The viscosity of the polymer solution increased with an increase in the polymer concentration. We grew hydrophilic and hydrophobic acrylic-resin coatings by ESD from the respective polymer solutions at various concentrations. For comparison, we also prepared the cast films from a 30 wt % hydrophilic resin/MeOH solution and 28 wt % hydrophobic resin/IPA solution, respectively. The cast films produced a native polymer surface.

Figures 1 and 2 show the surface SEM images of the hydrophilic and hydrophobic acrylic resin-coated

TABLE II
Properties of Poly(MMA-*co*-BMA-*co*-2-HEMA-*co*-MAA)/IPA Solution

Concentration (wt %)	Viscosity (mPas)	Surface tension (mN/m)	Conductivity (mS/m)
4	3.53	22.0	0.5
15	135	22.8	1.8
20	458	23.2	3.1
28	–	23.1	8.2

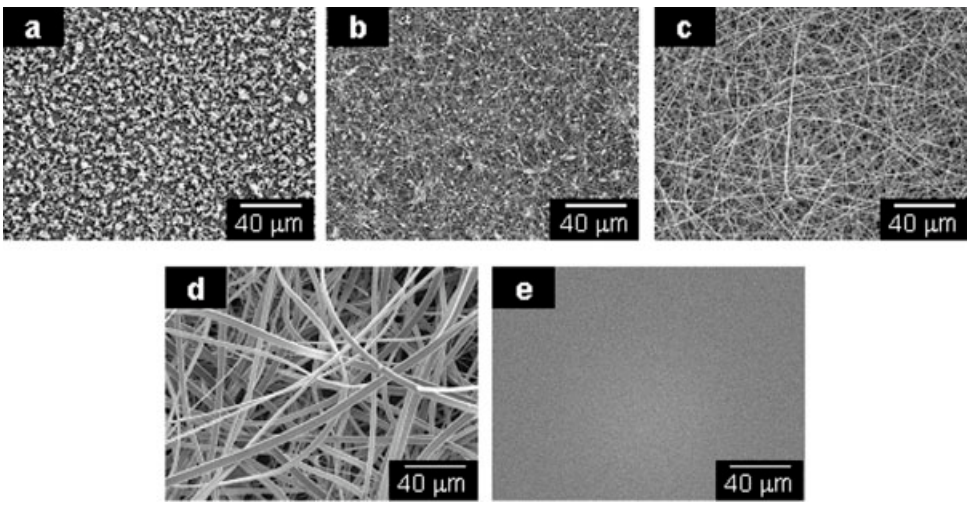

Figure 1 Surface SEM images of hydrophilic acrylic resin-coated layer; electrosprayed coatings from (a) 10 wt %, (b) 15 wt %, (c) 20 wt %, and (d) 30 wt % solutions, and (e) cast film from 30 wt % solution.

layers, respectively. The size of the structures in the coated layer is shown in Figure 3. At the lower solution viscosity, beads were formed. The solution with a higher viscosity tended to form a thicker ribbon-like fiber. These results correspond to the effect of the solution viscosity described in our previous article.[8,13] The average diameter of the spheres/fibers was 0.1–4 μm for the hydrophilic resin-coated layer and 5–15 μm for the hydrophobic resin-coated layer. On the other hand, the surfaces of the cast films were very smooth.

Figures 4 and 5 are photographs of 2 mg water droplets and the contact angles on the hydrophilic and hydrophobic acrylic resin-coated surfaces, respectively. All of the hydrophilic acrylic resin-coated surfaces by ESD showed a lower contact angle than that of the cast film [49°, Fig. 4(e)]. Particularly, the electrosprayed surfaces made from a 30 wt % hydrophilic acrylic resin solution is superhydrophilic, with a contact angle of 0° [Fig. 4(d)]. On the other hand, all of the hydrophobic acrylic resin-coated surfaces by ESD showed a larger contact angle than that of the cast film [73°, Fig. 5(e)]. These results indicate that ESD is a useful method for designing a textured surface and controlling the surface wettability.

Wetting behavior on microtextured surfaces by ESD

There are two well-established models for wetting on rough surfaces: the homogeneous wetting, where the liquid completely penetrates the roughness

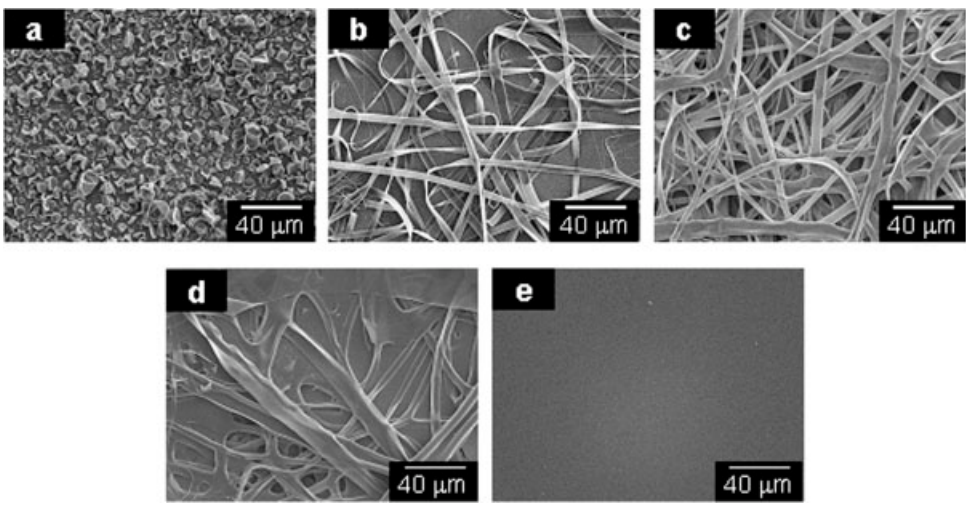

Figure 2 Surface SEM images of hydrophobic acrylic resin-coated layer; electrosprayed coatings from (a) 4 wt %, (b) 15 wt %, (c) 20 wt %, and (d) 28 wt % solutions, and (e) cast film from 28 wt % solution.

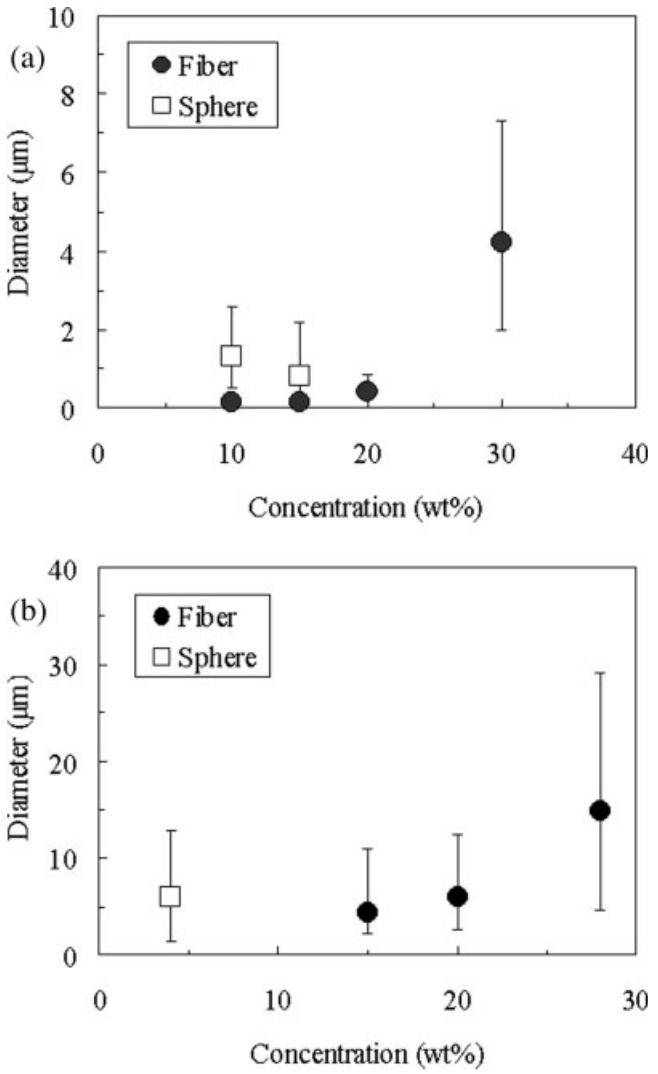

Figure 3 Diameter of fibers/spheres in (a) hydrophilic acrylic resin-coated layer, and (b) hydrophobic acrylic resin-coated layer.

grooves, and the heterogeneous wetting, where air is trapped underneath the liquid inside the roughness grooves. The apparent contact angle on a rough surface in the homogeneous regime, θ_W is given by the Wenzel equation[28]

$$\cos\ \theta_W = r\ \cos\ \theta_Y \tag{1}$$

where, θ_Y is the ideal Young contact angle and r is the roughness ratio, defined as the ratio of the true area of the solid surface to its projection area. This equation shows that, if a surface is hydrophilic ($\theta_Y < 90^\circ$), roughness ($r > 1$) makes θ_W smaller than θ_Y and *vice versa*. On the other hand, the apparent contact angle in the heterogeneous regime composed of two different materials, θ_{CB}, is given by the Cassie–Baxter equation[29]

$$\cos\ \theta_{CB} = f_1\ \cos\ \theta_1 + f_2\ \cos\ \theta_2 \tag{2}$$

where, a unit area of the surface has a surface area fraction f_1 with a contact angle θ_1 and an area fraction f_2 with a contact angle θ_2. When f_2 represents the area fraction of trapped air, eq. (2) can be modified as follows:

$$\cos\ \theta_{CB} = f\ \cos\ \theta_Y + (1-f)\cos\ 180^\circ = f\ \cos\ \theta_Y + f - 1 \tag{3}$$

where, f is an area fraction of the solid-liquid interface and $(1 - f)$ is that of the solid–air interface. This equation shows that, if a surface is hydrophobic ($\theta_Y > 90^\circ$), the increase in area fraction of trapped air makes θ_{CB} larger than θ_Y.

As shown in Figures 1 and 2, the surface morphologies of the electrosprayed surfaces composed of fibers and/or spheres were highly complicated. To understand the wetting behavior of water droplets on the electrosprayed surfaces, we calculated the apparent contact angle using a simple first-approximation theoretical model. To apply the Cassie–Baxter equation to our data, we need to know the area fraction of liquid–solid interface. The experimental measurement of the area fraction is very difficult. Therefore, in the present study, we adapted the Wenzel equation. The surface roughness, R_a, obtained from

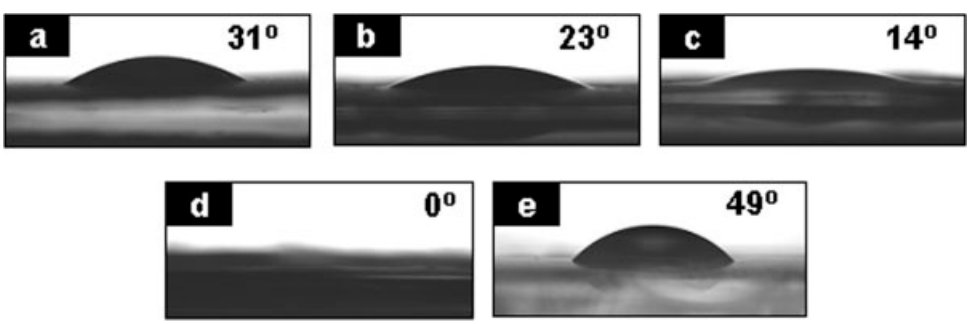

Figure 4 Shapes of 2 mg water droplets and contact angles on hydrophilic acrylic resin-coated surfaces; electrosprayed coatings from (a) 10 wt %, (b) 15 wt %, (c) 20 wt %, and (d) 30 wt % solutions, and (e) cast film from 30 wt % solution. All data were reproducible within 3 degrees.

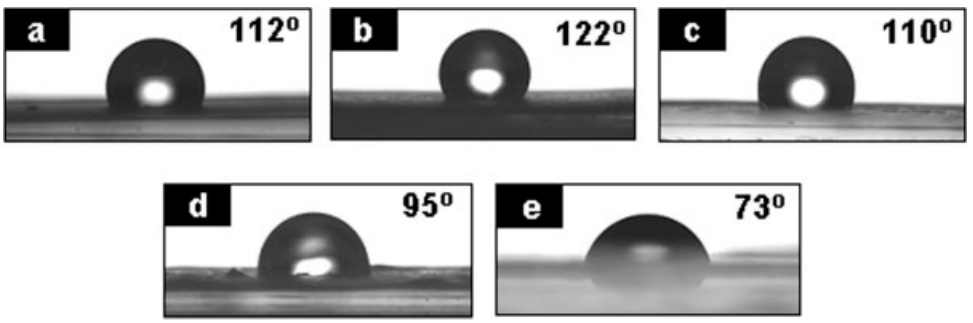

Figure 5 Shapes of 2 mg water droplets and contact angles on hydrophobic acrylic resin-coated surfaces; electrosprayed coatings from (a) 4 wt %, (b) 15 wt %, (c) 20 wt %, and (d) 28 wt % solutions, and (e) cast film from 28 wt % solution. All data were reproducible within 3 degrees.

the 3D profile observations of the electrosprayed surfaces and the contact angle of the cast film are represented by r and θ_Y in eq. (1), respectively. Here, R_a is an average deviation from the arithmetic centerline of the surface and used for simplification. Figure 6 shows the relationship between the surface roughness, R_a, and the contact angle on the electrosprayed surfaces. The theoretical results agreed well with the experimental ones for the hydrophilic resin-coated surfaces [Fig. 6(a)]. This suggests that the wetting behavior on the hydrophilic resin-coated surfaces obeys the Wenzel behavior. On the other hand, the distinct difference between the experimental result and theoretical one appears for the higher surface roughness on the hydrophobic resin-coated surfaces; the experimental contact angle is larger than the theoretical prediction based on the Wenzel equation [Fig. 6(b)]. This implies that the enhancement in the apparent contact angle attributed to the trapped air between water droplets and the textured surface. In other words, the wetting behavior appears to follow the Cassie–Baxter behavior.

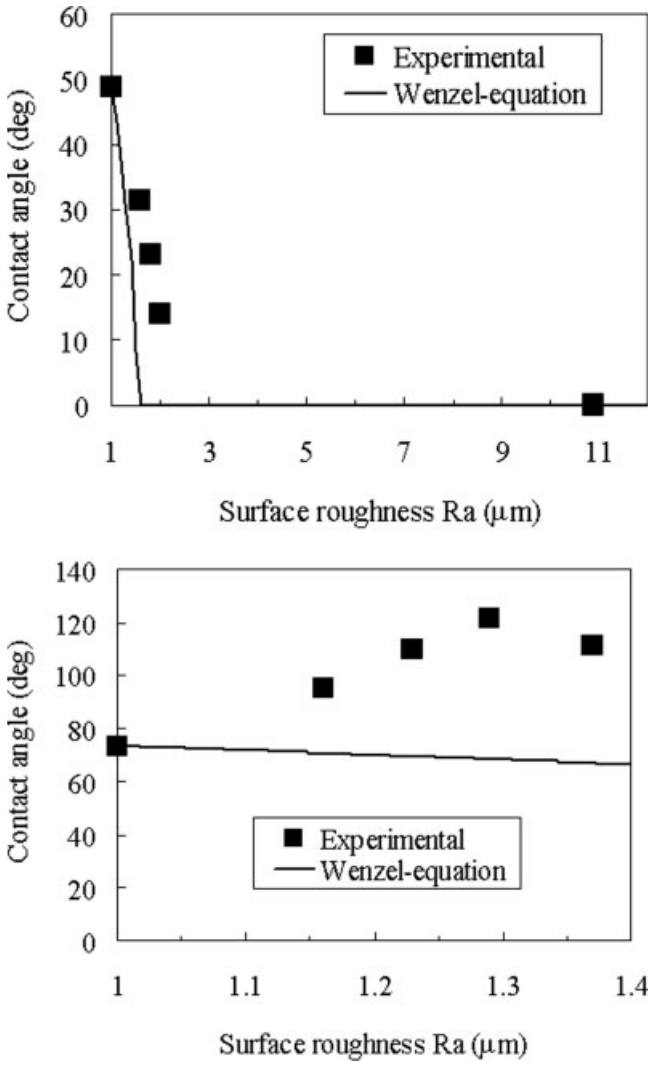

Figure 6 Relationship between surface roughness, Ra, and contact angle of water droplets on electrosprayed surfaces: (a) hydrophilic acrylic resin-coated layer, and (b) hydrophobic acrylic resin coated layer.

Wetting and sliding behaviors on patterned surface composed of aligned fibers by ESD

One of the recent breakthroughs in electrostatic fiber formation (or electrospinning) is the alignment of fibers.[4,5] Xia and Li have demonstrated that electrospun fibers could be uniaxially aligned over long length scales (up to several centimeters) by using a collector consisting of two pieces of conductive plates separated by a void gap.[30,31] Here, we obtained the aligned fibers from a 15 wt % hydrophobic resin/IPA solution by ESD using the gap method (The distance between the nozzle tip and the grounded two aluminum plates with a 10 cm gap was 15 cm. All other ESD conditions were the same as mentioned above); and then placed the aligned fibers on an aluminum substrate to produce a patterned surface. Figure 7(a) shows a typical SEM image of the patterned surface composed of the aligned fibers. This image clearly supported the fact that the ribbon-like fibers of the hydrophobic acrylic resin were uniaxially aligned on the substrate. The fiber diameter

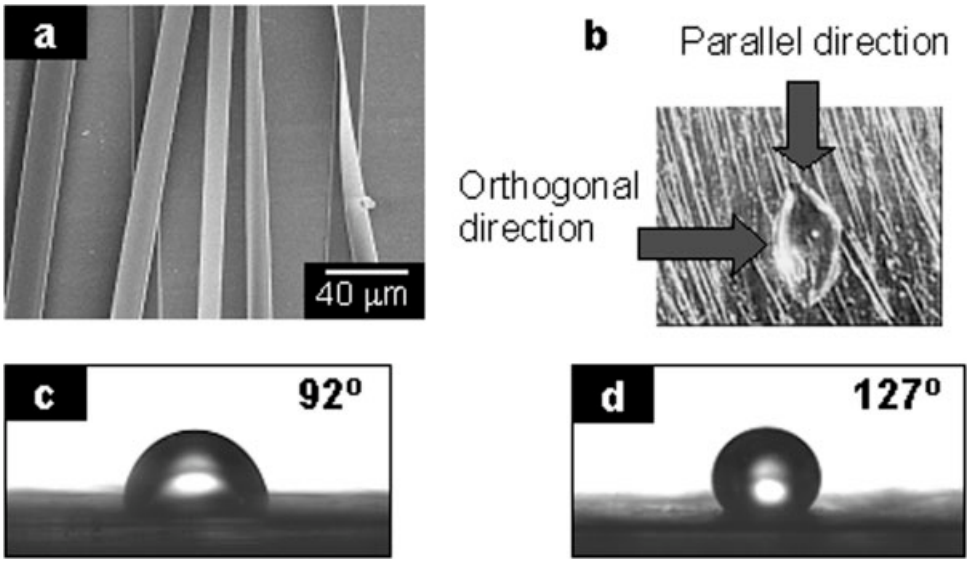

Figure 7 (a) SEM image of the patterned surface composed of aligned fibers by ESD. (b) Optical micrograph (top view) of wetting for a water droplet on the patterned surface by ESD and the measurement direction. Shapes of 2 mg water droplets on the patterned surface composed of aligned fibers by ESD, (c) from the orthogonal direction, and (d) from the parallel direction.

corresponded to that on the randomly deposited surface by ESD from the same polymer solution [see Fig. 2(b)] and average value of base × height obtained from the 3D profile observations was 6.5 μm × 1.1 μm. Figure 7(b) shows a typical optical micrograph of wetting for a water droplet on the patterned

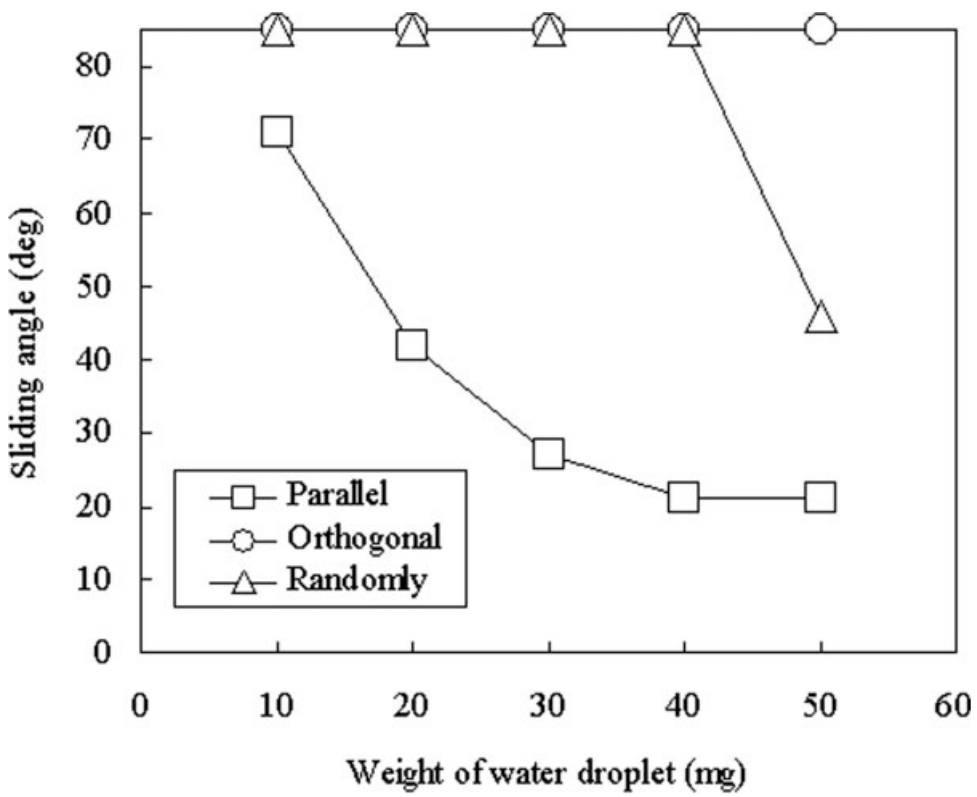

Figure 8 Effect of the weight of the water droplet on the sliding angles for the surfaces composed of electrosprayed fibers from 15 wt % hydrophobic acrylic-resin solution. (□) parallel direction in the patterned surface composed of uniaxially aligned fibers, (○) orthogonal direction in the patterned surface composed of uniaxially aligned fibers, and (△) on the surface composed of randomly deposited fibers.

surface and the measurement direction. The water contact angles on the patterned surface composed of aligned fibers were 127° and 92° from the parallel and orthogonal directions, respectively, [Fig. 7(c,d)]. The water contact angle from the parallel direction corresponded to that on the randomly deposited surface by ESD from the same polymer solution [122°, see Fig. 5(b)]. These results indicate that the patterned surface composed of aligned fibers shows anisotropy of the wetting behavior. Figure 8 shows the effect of the weight of the water droplet on the sliding angles. As shown in the figure, the sliding angle for the parallel direction in the patterned surface decreased with an increase in the weight of the water droplet. On the other hand, for the orthogonal direction in the patterned surface, water droplets with various weights did not slide down even at the maximum tilt angle (85°). These results indicate that the patterned surface also shows a strong sliding behavior anisotropy; the water droplet easily slides down in the parallel direction on the patterned surface, but hard to slide down in the orthogonal direction on the patterned surface. For the randomly fiber-deposited surface, only water droplet with highest weight can slide down. This result supported that patterned surface was very effective for preventing the orthogonal-direction sliding behavior.

CONCLUSIONS

Microtextured surfaces were prepared by ESD from hydrophilic and hydrophobic acrylic resin solutions. The wetting behaviors on the electrosprayed surfaces composed of fibers and/or spheres were influenced by both the chemical composition and surface roughness; the hydrophilicity and hydrophobicity on the electrosprayed surfaces were enhanced by increasing the surface roughness. Water contact angles on the electrosprayed surfaces from hydrophilic and hydrophobic resins changed with a maximum at about 50 degrees compared with their native smooth surfaces. Our first-approximation theoretical approach suggested that the wetting behaviors on the hydrophilic and hydrophobic resin-coated surfaces would be attributed to the Wenzel and Cassie–Baxter regimes, respectively. In addition, the patterned surface composed of aligned fibers by ESD showed anisotropy for both the wetting and sliding behaviors. These results indicate that ESD is a useful method for designing textured surfaces and controlling the surface wettability. Recently, Yamagata and coworkers reported the micropatterning by ESD and a stencil mask.[32] Precise control of nano-microtextured surfaces by the electrospray process opens a new direction for the electronic, optical, and medical applications.

The authors thank Mr. Yoshiaki Yanai, Kyowa Interface Science, and Mr. Yusuke Kuwahara, KEYENCE, for the sliding angle measurements and the laser profile microscope observations, respectively.

References

1. Salata, O. V. Curr Nanosci 2005, 1, 25.
2. Doshi, J.; Reneker, D. H. J Electrostat 1995, 35, 151.
3. Reneker, D. H.; Chun, I. Nanotechnology 1996, 7, 216.
4. Li, D.; Xia, Y. Adv Mater 2004, 16, 1151.
5. Dzenis, Y. Science 2004, 304, 1917.
6. Morozov, V. N.; Morozova, T. Anal Chem 1999, 71, 1415.
7. Uematsu, I.; Matsumoto, H.; Morota, K.; Minagawa, M.; Tanioka, A.; Yamagata, Y.; Inoue, K. J Colloid Interface Sci 2004, 269, 336.
8. Morota, K.; Matsumoto, H.; Mizukoshi, T.; Konosu, Y.; Minagawa, M.; Tanioka, A.; Yamagata, Y.; Inoue, K. J Colloid Interface Sci 2004, 279, 484.
9. Seo, H.; Matsumoto, H.; Hara, S.; Minagawa, M.; Tanioka, A.; Yamagata, Y.; Inoue, K. Polymer J 2005, 37, 391.
10. Matsumoto, H.; Wakamatsu, Y.; Minagawa, M.; Tanioka, A. J Colloid Interface Sci 2006, 293, 143.
11. Hoyer, B.; Sørensen, G.; Jensen, N.; Nielsen, D. B.; Larsen, B. Anal Chem 1996, 68, 3840.
12. Saf, R.; Goriup, M.; Steindl, T.; Hamedinger, T. E.; Sandholzer, D.; Hayn, G. Nat Mater 2004, 3, 323.
13. Matsumoto, H.; Mizukoshi, T.; Nitta, K.; Minagawa, M.; Tanioka, A.; Yamagata, Y. J Colloid Interface Sci 2005, 286, 414.
14. de Gennes, P. G.; Brochard-Wyart, F.; Quéré, D. Gouttes, Bulles, Perles et onde; Belin: Paris, 2002; Chapter 9.
15. Yan, H.; Kurogi, K.; Mayama, H.; Tsujii, K. Angew Chem Int Ed Engl 2005, 44, 3453.
16. Tadanaga, K.; Katata, N.; Minami, T. J Am Chem Soc 1997, 80, 1040.
17. Abdelsalam, M. E.; Bartlett, P. N.; Kelf, T.; Baumberg, J. Langmuir 2005, 21, 1753.
18. Morita, M.; Koga, T.; Otsuka, H.; Takahara, A. Langmuir 2005, 21, 911.
19. Jopp, J.; Grüll, H.; Yerushalmi-Rozen, R. Langmuir 2004, 20, 10015.
20. Lee, W.; Jin, M.-K.; Yoo, W. C.; Lee, J.-K. Langmuir 2004, 20, 7665.
21. Yoshimitsu, Z.; Nakajima, A.; Watanabe, T.; Hashimoto, K. Langmuir 2002, 18, 5818.
22. Feng, L.; Song, Y.; Zhai, J.; Liu, B.; Xu, J.; Jiang, L.; Zhu, D. Angew Chem Int Ed Engl 2003, 42, 800.
23. Jiang, L.; Zhao, Y.; Zhai, J. Angew Chem Int Ed Engl 2004, 43, 4338.
24. Acatay, K.; Simsek, E.; Ow-Yang, C.; Menceloglu, Y. Z. Angew Chem Int Ed Engl 2004, 43, 5210.
25. Stegmaler, T.; Dauner, M.; Dinkelmann, A.; Scherrieble, A.; von Arnim, V.; Schneider, P.; Planck, H. Tech Text 2004, 47, 142.
26. Ma, M.; Hill, R. M.; Lowery, J. L.; Fridrikh, S. V.; Rutledge, G. C. Langmuir 2005, 21, 5549.
27. Ma, M.; Mao, Y.; Gupta, M.; Gleason, K. K.; Rutledge, G. C. Macromolecules 2005, 38, 9742.
28. Wenzel, R. N. Ind Eng Chem 1936, 28, 988.
29. Cassie, A. B. D.; Baxter, S. Trans Faraday Soc 1944, 40, 546.
30. Li, D.; Wang, Y.; Xia, Y. Nano Lett 2003, 3, 1167.
31. Li, D.; Wang, Y.; Xia, Y. Adv Mater 2004, 16, 361.
32. Kim, J. W.; Yamagata, Y.; Kim, B.; Higuchi, T. In Proceedings of Technical Digest of 17th IEEE International Conference on MEMS; Maastrichit, Netherlands, January 25–29, 2004; p 625.